



ELSEVIER

Available online at [www.sciencedirect.com](http://www.sciencedirect.com)**ScienceDirect**journal homepage: [www.elsevier.com/locate/he](http://www.elsevier.com/locate/he)

# A first principles study of hydrogen storage on lithium decorated two dimensional carbon allotropes



CrossMark

**Shwetank Yadav, Jasmine Tam, Chandra Veer Singh\***

Department of Materials Science and Engineering, University of Toronto, 184 College Street, Suite 140, Toronto, Ontario M5S 3E4, Canada

---

## ARTICLE INFO

**Article history:**

Received 8 August 2014

Received in revised form

25 January 2015

Accepted 9 March 2015

Available online 2 April 2015

**Keywords:**

Hydrogen storage

Graphyne

Carbon allotropes

Density functional theory

Physisorption

---

## ABSTRACT

Graphene has been intensively investigated as a possible hydrogen storage medium due to the spectacular properties granted by its two-dimensional nature. Since graphene's discovery, several new two-dimensional carbon allotropes have been theorized and synthesized. We investigated the hydrogen storage ability of six such allotropes:  $C_{65}$ ,  $C_{64}$ ,  $C_{63}$ ,  $C_{62}$ ,  $C_{31}$  and  $C_{41}$ . The ability to anchor lithium metal atoms over each allotrope and the hydrogen binding energies for each lithium decorated allotrope were studied with density functional theory using LDA, GGA and vdW-DF2 (for describing van der Waals interactions) functionals. All the allotropes were able to achieve double sided lithium decoration and hydrogen adsorption. Every allotrope other than  $C_{31}$  possessed lithium binding energies stronger than bulk lithium's cohesive energy which indicates that adsorbed lithium atoms will not cluster on the allotrope surface. Furthermore, every structure produced hydrogen binding energies stronger than that of lithium decorated graphene, suggesting the potential of use of these structures in practical hydrogen storage media. The  $C_{41}$  structure was able to adsorb far more hydrogen molecules than any other structure with a maximum hydrogen gravimetric density of 7.12 wt.% using the vdW-DF2 functional.

Copyright © 2015, Hydrogen Energy Publications, LLC. Published by Elsevier Ltd. All rights reserved.

---

## Introduction

In recent years, the numerous environmental issues presented by fossil fuels have acted as a major driving force for the research community to place focus on greener and more sustainable alternatives. Among the many energy sources being investigated at the moment are hydrogen fuels as they do not create any carbon emissions when used to produce

energy [1]. One obstacle that researchers face with regards to hydrogen fuels is finding a method to effectively store hydrogen prior to fuel consumption. The US Department of Energy has set a target to achieve 5.5 wt% gravimetric density for hydrogen storage in light-duty vehicles by 2015 [2]. Conventional technologies have been unable to meet these targets in a safe and practical manner [3]. Hydrogen adsorption on substrates has been explored as a possible route towards meeting these storage goals [4], including the use of materials

\* Corresponding author. Tel.: +1 (416) 946 5211; fax: +1 (416) 978 4155.

E-mail address: [chandradeep.singh@utoronto.ca](mailto:chandradeep.singh@utoronto.ca) (C.V. Singh).  
<http://dx.doi.org/10.1016/j.ijhydene.2015.03.038>

0360-3199/Copyright © 2015, Hydrogen Energy Publications, LLC. Published by Elsevier Ltd. All rights reserved.

such as metal organic frameworks [5], carbon nanotubes [6] and boron nitride sheets [7] and fullerenes [8]. Among carbon based substrate materials, two-dimensional graphene has been found to be particularly promising [9]. Graphene's high specific surface area in addition to its unique mechanical and electronic properties allow it to be an ideal substrate which can be modified through metal decoration for increased hydrogen adsorption [10].

Since the discovery of graphene several other two dimensional carbon structures, such as graphyne [11,12] and graphdiyne [13], have been synthesized or theorized. These monolayer materials show promise for hydrogen storage applications. For example, in a study by Zhang et al. [14] lithium decorated graphyne was predicted to have a gravimetric density of 15.15 wt%, higher than that of graphene. In 2013, Lu et al. [15] theoretically predicted four new two-dimensional carbon structures which are mechanically stable at room temperature. These new carbon allotropes, along with graphyne and another proposed carbon allotrope called graphylene [16], have different carbon bond hybridizations and electron density distributions than graphene. This may give them potential to better interact with and bind metal adatoms and hydrogen molecules, as graphyne has already been predicted to do [14].

The present study investigated the hydrogen storage ability with metal decoration of the six carbon allotropes discussed by Lu et al. [15], which according to the naming convention followed by them are:  $C_{65}$ ,  $C_{64}$  (graphylene),  $C_{63}$ ,  $C_{62}$  (graphyne),  $C_{31}$  and  $C_{41}$ . The  $C_{6n}$  structures consist of hexagons connected by  $n$ -sided polygons, going from a pentagon for  $n = 5$  to a triangle for  $n = 3$  and a straight chain of two carbon atoms for  $n = 2$ . Similarly the  $C_{31}$  and  $C_{41}$  structures consist of triangles and squares connected by single carbon  $C_1$  units. Three of the new structures ( $C_{65}$ ,  $C_{63}$  and  $C_{41}$ ) are considered more stable than graphyne and the fourth ( $C_{31}$ ) is just barely less stable. The lithium binding ability for each of these structures was investigated, with lithium being selected for metal decoration as it is the lightest known metal and so would help increase relative hydrogen mass in the system. The maximum hydrogen gravimetric density was also investigated by adsorbing multiple hydrogen molecules on the lithium-decorated structures.

Another issue associated with most theoretical predictions of hydrogen adsorption on metal-decorated carbon-based structures is that they utilize density functional theory (DFT) with local density approximation (LDA) and generalized gradient approximation (GGA) functionals. For example, the previously mentioned study by Zhang et al. [14] of lithium decorated graphyne utilized LDA. However, the LDA functional can be quite inaccurate for such complex systems and will often overpredict adsorption strength. On the other hand, while the GGA functional models covalent type forces well, it poorly represents van der Waals (vdW) interactions. Such vdW interactions are significant in describing the weak physisorption type of bonding typical of molecular hydrogen adsorption on carbon substrates [17,18] and the interaction between neighboring metal atoms especially at higher coverages [18]. The more recently implemented vdW-DF2 [19] functional is said to better account for vdW forces [20] and so should provide more accurate adsorption energies. Hence,

this study compares theoretical predictions for lithium and hydrogen adsorption energies using the LDA, GGA and vdW-DF2 functionals for each simulation.

## Computational details

The various carbon allotrope systems were studied using first principles calculations through density functional theory (DFT) as implemented using the plane-wave pseudopotential approach in Quantum Espresso [21]. In order to ascertain accuracy and the effect of different functionals, three electron exchange functional types were used. The local density approximation (LDA) functional was described using the Perdew-Wang method [22]. The generalized gradient approximation (GGA) functional was described using the Perdew-Burke-Ernzerhof (PBE) [23] method. The vdW-DF2 functional [19] was used to better describe van der Waals forces. This functional improves on the earlier vdW-DF [24] by replacing its revPBE semi-local exchange functional with PW86 and using an improved large-N expansion asymptotic gradient correction for the long-range nonlocal component of exchange-correlation energy. This results in increased accuracy in estimating equilibrium separations,  $H_2$  bond strengths and van der Waals attraction at intermediate separations longer than equilibrium ones [19]. Ultrasoft pseudopotentials were used for GGA and vdW-DF2 calculations, while norm-conserving pseudopotentials were used for the LDA calculations. The kinetic energy cutoff value was set to 60 Ry (1 Ry  $\sim$  13.606 eV) for the wave functions and to 600 Ry for the charge density. The Brillouin zone was sampled using a  $8 \times 8 \times 1$  Monkhorst-Pack [25] k-point grid and Methfessel-Paxton [26] smearing of 0.01 Ry [27]. The supercell and atomic positions were optimized using the conjugate gradient (CG) algorithm. The total energy convergence was converged to within less than 5 meV/atom. Each of the structures were modeled using periodic supercells of 48 carbon atoms, except for the  $C_{65}$  supercell which had 40 carbon atoms. Each system had a vacuum layer thickness of more than 30 Å.

The average binding energy for a metal atom was calculated through the following equation:

$$E_b = -[E_{\text{carbon}+n\text{metal}} - (E_{\text{carbon}} + nE_{\text{metal}})]/n \quad (1)$$

where  $E_{\text{carbon}+n\text{metal}}$  is the total energy of the metal decorated carbon allotrope system,  $E_{\text{carbon}}$  is the energy of the carbon allotrope sheet alone,  $E_{\text{metal}}$  is the total energy of the free metal adatom and  $n$  corresponds with the number of metal adatoms.

Consequently, the average binding energy for hydrogen adsorption on the lithium-decorated carbon allotropes can be calculated through the following equation:

$$E_b = -[E_{\text{metal-carbon}+iH_2} - (E_{\text{metal-carbon}} + iE_{H_2})]/i \quad (2)$$

where  $E_{\text{metal-carbon}+iH_2}$  is the total energy of the metal decorated carbon allotrope system with hydrogen adsorbed,  $E_{\text{metal-carbon}}$  is the total energy of the metal decorated carbon allotrope sheet,  $E_{H_2}$  is the total energy of the free  $H_2$  molecule and  $i$  corresponds to the number of  $H_2$  molecules. A positive binding energy in the previous two equations indicates a stable system configuration.

The charge density differences were obtained from the following equation:

$$\Delta\rho = \rho_{\text{metal-carbon+iH}_2} - (\rho_{\text{metal-carbon}} + \rho_{\text{iH}_2}) \quad (3)$$

where  $\rho_{\text{metal-carbon+iH}_2}$  is the charge density of the metal decorated carbon allotrope system with hydrogen adsorbed,  $\rho_{\text{metal-carbon}}$  is the charge density of the metal decorated carbon allotrope sheet and  $\rho_{\text{iH}_2}$  is the charge density of the  $\text{iH}_2$  molecules in their adsorbed positions.

## Results and discussion

### Metal adsorption

As previously reported, metal decoration on graphene greatly enhances its limited hydrogen adsorption ability as the hydrogen molecules bind to the metal atoms rather than the carbon substrate [10]. Hence, double sided lithium decoration was conducted for each carbon substrate to increase the maximum possible hydrogen storage ability. Lithium was selected as the metal adatom as it is the lightest metal and hence it would create a relatively lower non-hydrogen mass fraction in the system. The multiple adsorption positions and system configurations investigated are illustrated in Fig. 1. The adsorption positions are above the center of various polygon shapes formed by carbon atoms in the plane of the various structures; these include a triangle site for the  $\text{C}_{31}$  surface, a square site for  $\text{C}_{41}$ , a hexagon site for  $\text{C}_{62}$ , hexagon and triangle sites for  $\text{C}_{63}$ , hexagon and square sites for  $\text{C}_{64}$  and hexagon and pentagon sites for  $\text{C}_{65}$ . Generally positions in the

large hollow rings of several of the structures (such as in the center of  $\text{C}_{64}$ ) were not investigated as they were presumed to produce weak lithium binding due to the large distance from surrounding atoms, based on previous work with graphene systems with similar large hollow spaces [28]. The lithium binding energies for these systems are displayed in Table 1 and Fig. 2 for easy comparison. All of the positions show positive stable binding energies, indicating that double sided lithium decoration is physically feasible. Furthermore, all structures except  $\text{C}_{31}$ , display lithium binding energies greater than the cohesive energy for bulk lithium (1.63 eV) and so should have well dispersed lithium atoms which avoid clustering. The  $\text{C}_{31}$  structure stands out by having a metal binding energies significantly below the others. In fact, its binding energy values (0.964, 0.687 & 0.420 eV for LDA, GGA and vdW-DF2 respectively) are below the bulk cohesive energy, indicating that lithium atoms are likely to cluster into agglomerates by migrating across the  $\text{C}_{31}$  surface. Adatom clustering due to low metal binding energy has been a problem in previous metal decoration systems [29]. Therefore, our results show that the studied  $\text{C}_{31}$  is not a good candidate for practical hydrogen storage. Nevertheless, it may still be possible to prevent lithium clustering by anchoring the metal adatoms on a vacancy, as has been previously suggested for other systems [29]. Overall, these results suggest that the remaining allotropes are more viable candidates for use in a practical storage device.

The Li binding energies for the  $\text{C}_{65}$  allotrope are the highest among the studied structures (from 3.348 eV with LDA at its strongest down to 2.203 eV with vdW-DF2), while the remaining allotropes show more or less similar binding energies (with the exception of  $\text{C}_{31}$  as discussed previously). For

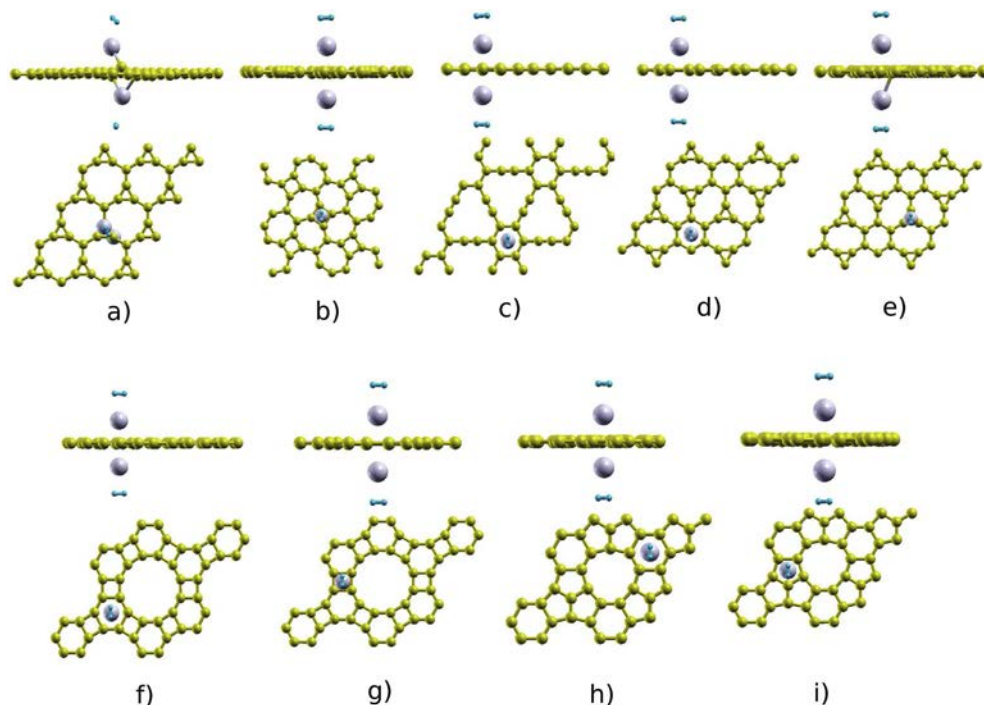


**Fig. 1 – Substrate structures and hydrogen adsorption sites of the six studied two-dimensional carbon allotropes with double-sided lithium decoration: a)  $\text{C}_{31}$ ; b)  $\text{C}_{41}$ ; c)  $\text{C}_{62}$ ; d)  $\text{C}_{63}$  hexa; e)  $\text{C}_{63}$  tri; f)  $\text{C}_{64}$  hexa; g)  $\text{C}_{64}$  square; h)  $\text{C}_{65}$  hexa; i)  $\text{C}_{65}$  penta.**

**Table 1 – Average lithium adsorption energy (eV) for each two-dimensional carbon allotrope and adsorption position. Note the bulk cohesive energy for lithium is 1.63 eV. All structures except C<sub>31</sub> possess lithium binding energy greater than the cohesive energy and this should prevent metal atom agglomeration.**

	C <sub>65</sub>		C <sub>41</sub>		C <sub>63</sub>		C <sub>64</sub>		C <sub>62</sub>		C <sub>31</sub>
	Hexa	Penta	Square	Hexa	Tri	Hexa	Square	Hexa	Tri	Hexa	Tri
LDA	3.348	3.341	2.678	2.524	2.261	2.688	2.678	2.462	0.964		
GGA	2.538	2.526	2.106	2.121	1.869	2.225	2.113	2.015	0.687		
vdW-DF2	2.203	2.210	1.775	1.791	1.618	1.859	1.798	1.696	0.420		

all allotropes, a specific pattern can be observed for the energies produced when using different exchange correlation functionals. The LDA functional consistently produces the highest lithium binding energy, followed by the GGA functional and the vdW-DF2 functional produces the lowest binding energy for each allotrope system. The vdW-DF2 functional is known to have a stronger repulsion for electron exchange effects than PBE GGA [30] and this is likely contributing to its relative lower metal adsorption energies. It is interesting to note that all the GGA and vdW-DF2 lithium binding energies are stronger than the corresponding lithium binding energies for double sided decoration on graphene [31], suggesting metal decoration for these structures might be more favorable than for graphene.

In order to understand the nature of bonding in the systems, the projected density of states (PDOS) for each of the metal decorated carbon allotropes simulated with the vdW-DF2 functional are presented in Fig. 3. For structures with multiple adsorption positions, only one PDOS diagram is shown for the position with the strongest binding energy as the other positions are likely to have very similar states. The carbon substrates clearly show sp hybridization within the carbon sheet where the carbon s and p shell peaks overlap in each diagram. The lithium atoms have very localized peaks which overlap with carbon peaks to some degree in all the structures and so there is likely some degree of hybridization between the lithium orbitals and surrounding carbon orbitals. The C<sub>65</sub> structure shows the highest degree of hybridization as the two lithium peaks line up very well with corresponding carbon peaks; in fact the red carbon p-orbital peak which overlaps the rightmost green lithium peak is barely visible. This indicates a strong degree of hybridization for the C<sub>65</sub>

structure and explains its stronger lithium binding energies. The C<sub>65</sub> structure also has the fewest zero state energy regions or number of deep valleys which are close to zero value in density of states, indicating it has a greater degree of delocalization of the electrons which are shared well amongst the system atoms and demonstrates that the lithium atoms have integrated well into the substrate system. Conversely, the C<sub>31</sub> structure displays the greatest number of deep valleys and has several energy regions with zero or near zero states. This indicates a greater degree of localization of electrons on atoms and decreased charge sharing within the system, indicating that the lithium adsorption is less favorable for the C<sub>31</sub> system configuration. The PDOS diagrams also demonstrate that none of the lithium adsorbed structures have a band gap, unlike the bare substrates where the C<sub>62</sub> and C<sub>64</sub> structures have small energy band gaps indicating they are semiconductors [15]. On the other hand, the adsorption of lithium seems to have metalized all the allotropes which all now display conductor like PDOS.

### Hydrogen adsorption

Following lithium adsorption, a hydrogen molecule was adsorbed on each lithium atom for all the carbon allotrope structures. The average hydrogen molecule binding energy (eV/H<sub>2</sub>) results are given in Table 2. The optimized configurations of the adsorbed hydrogen molecules for each position can be seen in Fig. 1. Unlike the lithium adsorption simulations, there is no clear pattern among the binding energies produced by the different exchange correlation functionals for hydrogen adsorption. In most cases (seven out of nine) the LDA functional produces the highest binding energy while the lowest binding energies are almost equally split between GGA and vdW-DF2 functionals. Overall, the C<sub>31</sub> allotrope displays much stronger binding energy than the other structures, opposite to its behavior for lithium adsorption, as can be seen in Fig. 4 for easy comparison. As the Li decorated C<sub>31</sub> structure was found to be relatively less stable (with a lithium binding energy even less than bulk lithium's cohesive energy), the addition of the hydrogen molecule's charge acts as a stabilizing force and makes the molecule's charge quite attractive to the lithium-C<sub>31</sub> system, thereby enhancing its adsorption energy. Amongst the remaining structures, the GGA and vdW-DF2 functionals produce roughly similar energies across all positions. The H<sub>2</sub> adsorption energies with LDA functional show greater variability, being fairly high for the C<sub>62</sub> allotrope (0.434 eV) and low for the C<sub>64</sub>-square position (0.089 eV). The vdW-DF2 functional displays the smallest variability for non-C<sub>31</sub> binding energies, with all of them having values within 0.02 eV of each other.

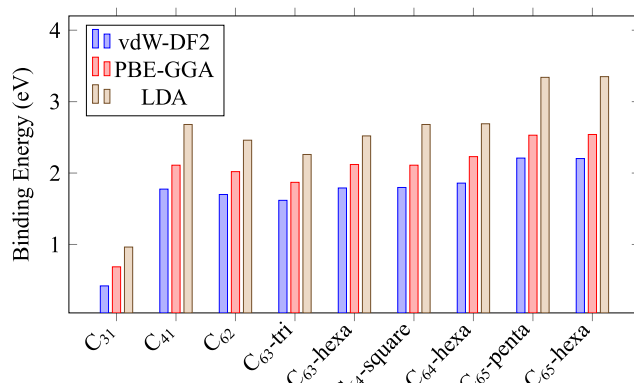


**Fig. 2 – Average metal binding energies (eV/atom) at multiple sites for the six studied two-dimensional carbon allotropes with double-sided lithium decoration.**

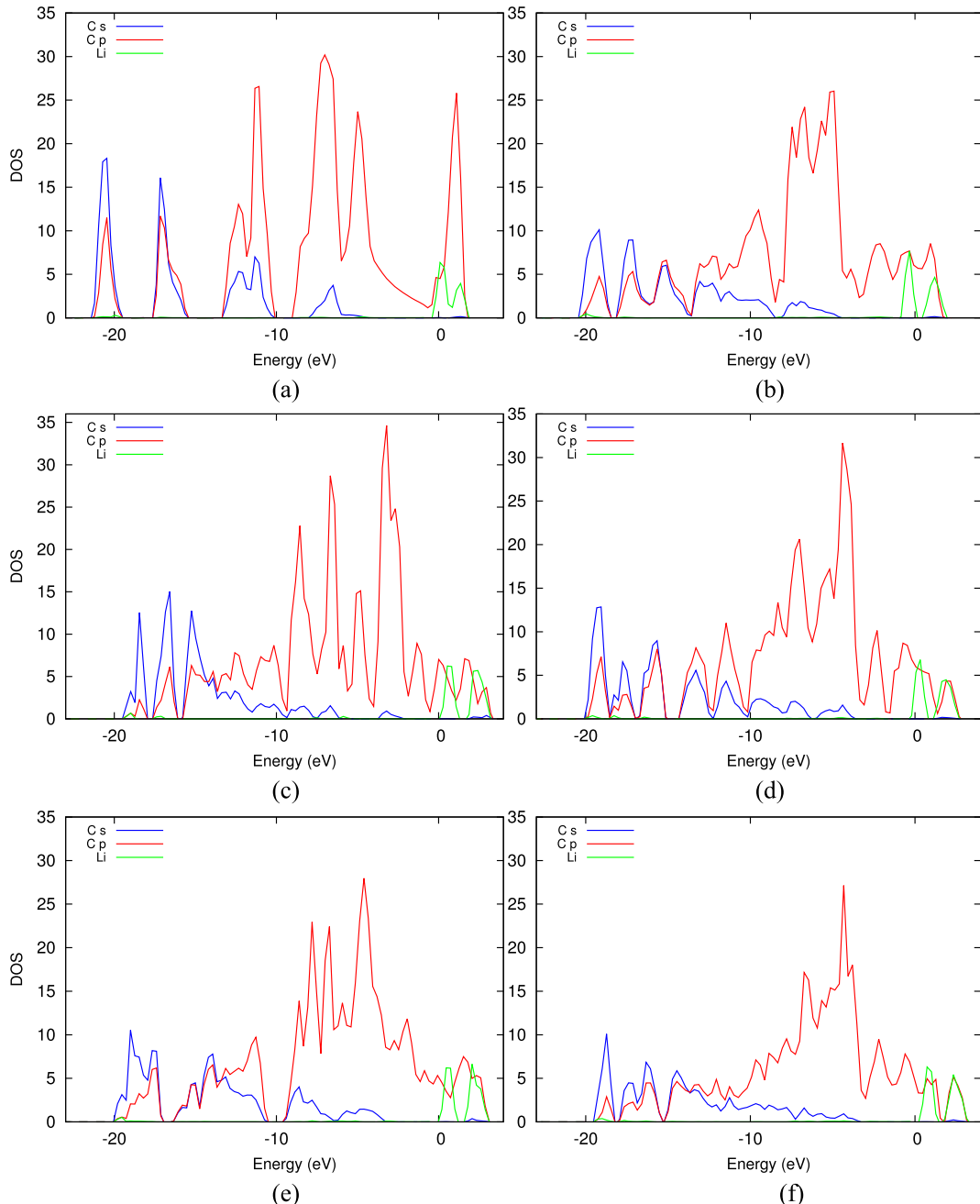


**Fig. 3 – Projected density of states (PDOS) for the lithium decorated two-dimensional carbon allotropes from simulations using the vdW-DF2 functional: a)  $C_{31}$ ; b)  $C_{41}$ ; c)  $C_{62}$ ; d)  $C_{63}$ ; e)  $C_{64}$ ; f)  $C_{65}$ . There is evidence of  $sp$  hybridization within the carbon sheet and hybridization between the lithium and carbon atoms. The  $C_{65}$  structure displays the greatest degree of hybridization and electron sharing while the  $C_{31}$  structure displays the highest localization of electrons.**

There also seems to be little relation between the strength of hydrogen adsorption and lithium adsorption behavior for the non- $C_{31}$  allotropes. Instead, the particular electronic and structural properties of each structure determine their interaction with the hydrogen molecules and a specific pattern seems to be difficult to predict *a priori*. Hence, it is not possible to determine the effect of hybridization between the lithium and carbon atoms on hydrogen storage capacity as other factors can play a more significant role for such relatively weak physisorption type binding. In a broad sense, positions

located in larger polygons such as hexagons or pentagons produced slightly stronger hydrogen binding than those in smaller polygons such as squares or triangles, although the magnitude of the difference is negligible (especially for vdW-DF2 results as pointed out). Interestingly, all the vdW-DF2 hydrogen adsorption energies are stronger than that of graphene with double sided lithium decoration with the same functional, while all the GGA binding energies are weaker (with the exception of  $C_{31}$ ) [31]. This once again points to the importance of considering vdW effects, where their neglect

**Table 2 – Average hydrogen adsorption energies (eV/H<sub>2</sub>) for each two-dimensional carbon allotrope and adsorption position.**

	C <sub>65</sub>		C <sub>41</sub>		C <sub>63</sub>		C <sub>64</sub>		C <sub>62</sub>		C <sub>31</sub>
	Hexa	Penta	Square	Hexa	Tri	Hexa	Square	Hexa	Tri	Hexa	
LDA	0.197	0.192	0.196	0.243	0.237	0.226	0.089	0.434	0.709		
GGA	0.158	0.161	0.159	0.179	0.179	0.167	0.167	0.194	0.743		
vdW-DF2	0.188	0.175	0.173	0.182	0.177	0.183	0.173	0.189	0.671		

leads to the conclusion that these carbon allotropes are inferior to graphene for hydrogen adsorption while their inclusion results in the opposite conclusion.

As all of the hydrogen molecules remained intact after adsorption and as all of the average hydrogen binding energies were below 1.0 eV, the hydrogen likely bonded with the lithium adatoms through physisorption. This is further confirmed by the charge density differences (CDD) of the systems for hydrogen adsorption, as seen in Fig. 5 for vdW-DF2 results. All of the structures follow the same pattern where there are very clear regions of charge accumulation and depletion on either side of the hydrogen molecules, indicating strong polarization of the hydrogen. This suggests that the hydrogen binds by a weak electrostatic dipole mechanism for all of the systems and there is no covalent character bonding or strong hybridization between the hydrogen and lithium atoms. Such relatively weak binding is actually advantageous as it allows easier release of the hydrogen molecules from the system while stronger covalent type bonds require significant input of energy.

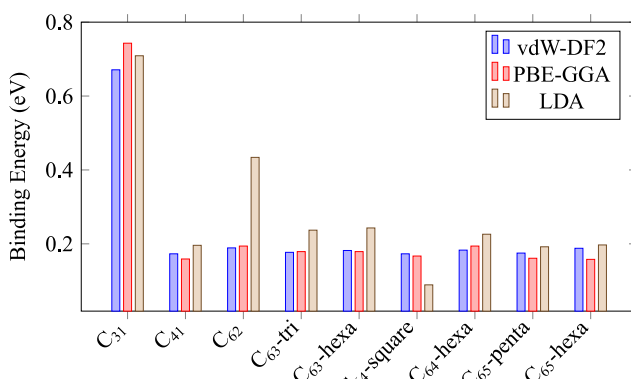
#### Maximum gravimetric density

The various structures were next investigated for adsorption of the highest number of hydrogen molecules they could accommodate. The C<sub>31</sub> structure was excluded from this study as it was not considered practical based on metal anchoring ability as previously discussed. Furthermore, since the vdW-DF2 functional is considered to be more accurate for hydrogen adsorption [31], the simulations were carried out with this functional alone. The systems analyzed so far had only four hydrogen atoms on two lithium atoms in 48 or 40 carbon atom substrates, leading to quite low gravimetric density for hydrogen (0.68–0.81 wt.%). However, even adding

multiple hydrogen molecules to each lithium atom would not be able to compensate for the large number of carbon atoms which represent a significant non-hydrogen mass fraction. Indeed, it can be seen from Fig. 1 that only a small area of the carbon substrate in each simulation is being used for hydrogen adsorption (assuming all such adsorption only occurs on lithium atoms). Hence, increasing the number of adsorbed lithium positions within each supercell would go towards greatly increasing hydrogen mass fraction in the supercell.

Expectedly, increasing the number of lithium atoms in each supercell caused the hydrogen binding energy to decrease and eventually made hydrogen adsorption unstable in the system. This is similar to a trend observed for nickel decorated graphene in our previous work [31], where increased metal coverage decreased the hydrogen adsorption energies. Several configurations with adsorption of lithium atoms at different positions were analyzed for different allotropes. The best results were obtained for the C<sub>64</sub> and C<sub>41</sub> structures. The C<sub>64</sub> was able to adsorb up to four lithium atoms in its 48 carbon supercell, meaning that it could accommodate double sided lithium decoration at only one additional position (another hexa position) compared to the earlier simulation. Each of the lithium atoms was able to adsorb only two hydrogen molecules to give a total of eight hydrogen molecules in the system, as seen in Fig. 6, which produced a hydrogen gravimetric density of 2.6 wt.%. The average binding energy per molecule for these 8 hydrogen molecules was 0.147 eV, a slight decrease from 0.183 eV binding energy for the initial system with lithium adsorbed at only one position.

The C<sub>41</sub> structure was able to adsorb lithium atoms at three additional positions within its 48 atom supercell, giving it a total of 8 adsorbed lithium atoms. Each of these in turn were able to adsorb a maximum of 3 hydrogen molecules, resulting in a total of 24 hydrogen molecules being successfully adsorbed in the supercell, as seen in Fig. 7. This produced a hydrogen gravimetric density of 7.12 wt.%, by far the highest of any of the carbon allotrope structures studied and the only one to exceed the DOE target of 5.5 wt.%. The average hydrogen binding energy per molecule was reduced to 0.087 eV, a marked decrease from the 0.173 eV energy for the initial single site adsorption case. Although the C<sub>41</sub> structure's gravimetric density is lower than the extremely high density of 15.15 wt% reported by Zhang et al. [14], it should be noted that the previous study used the LDA functional which is less accurate than the vdW-DF2 functional we have utilized and often overpredicts binding energies. Indeed, in a previous study we have reported that using the newer vdW-DF2 functional produces drastically lower hydrogen gravimetric density for graphene (6.12 wt.% at best) compared to earlier

**Fig. 4 – Average hydrogen binding energies (eV/H<sub>2</sub>) at multiple sites for double sided lithium decorated carbon allotrope systems.**

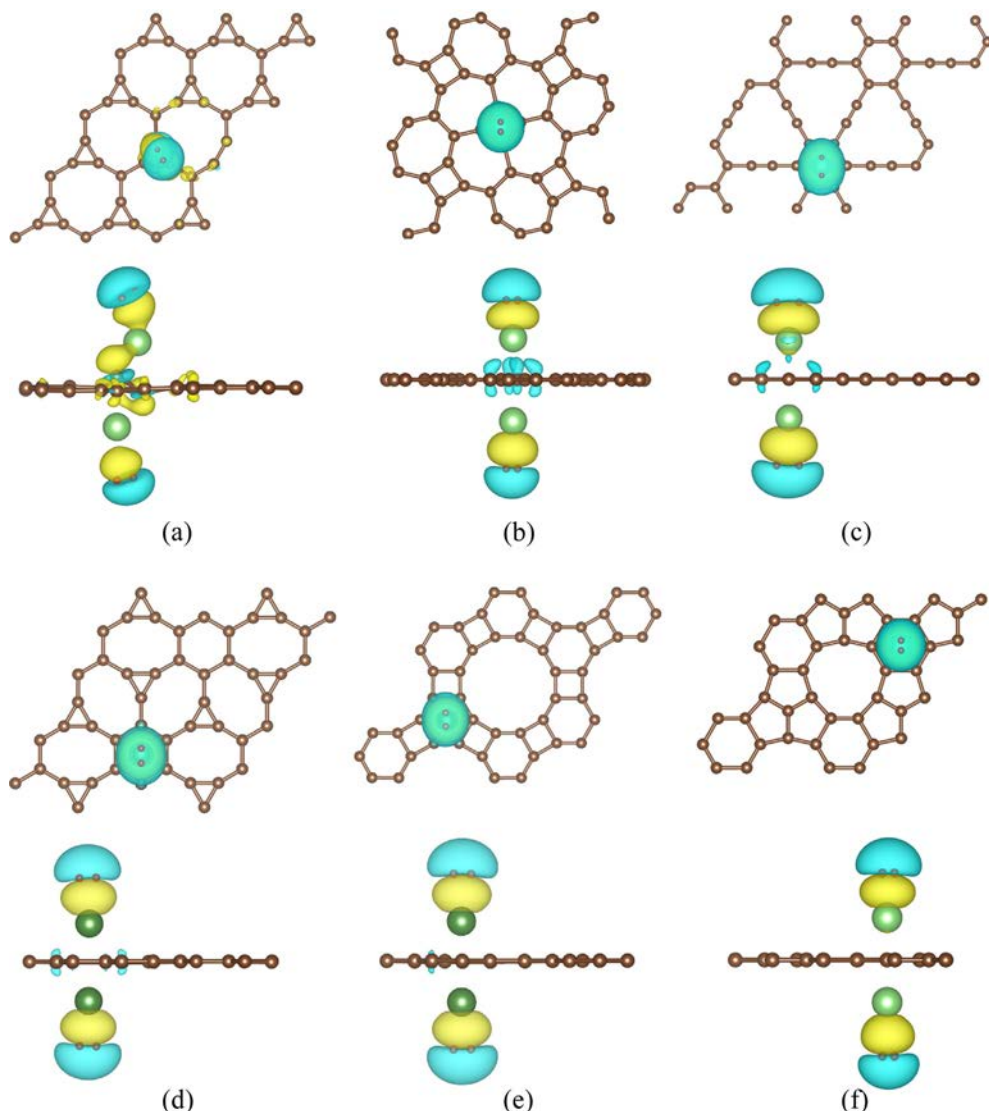


**Fig. 5 – Charge density difference isosurfaces for (a)  $C_{31}$ , (b)  $C_{41}$ , (c)  $C_{62}$ , (d)  $C_{63}$ -hexa, (e)  $C_{64}$ -hexa and (f)  $C_{65}$ -hexa systems. Yellow indicates regions of charge gain, blue indicates regions of charge loss, green indicates lithium atoms and red indicates hydrogen atoms. The isosurfaces show clear polarization around the hydrogen molecules. (For interpretation of the references to color in this figure legend, the reader is referred to the web version of this article.)**

studies which used LDA (with a value reported up to 16 wt.%) [31]. Hence, the  $C_{41}$  structure demonstrates higher possible hydrogen gravimetric density than graphene. This also demonstrates the importance of selecting a proper exchange

correlation functional which can represent weak van der Waals interactions for molecular hydrogen systems.

The geometry of the  $C_{41}$  structure likely plays a role in its outstanding performance. The structure has less large open



**Fig. 6 – Configuration of  $C_{64}$  system with maximum number of adsorbed hydrogen molecules. Each lithium atom binds two hydrogen molecules to give eight molecules in the system and a hydrogen gravimetric density of 2.6 wt%.**

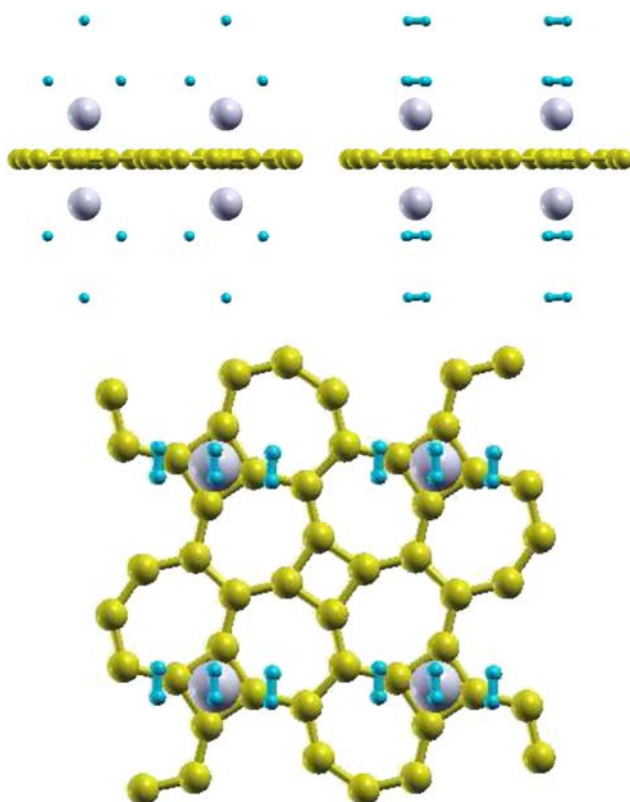


**Fig. 7 – Configuration of  $C_{41}$  system with maximum number of adsorbed hydrogen molecules. Each lithium atom binds three hydrogen molecules to give twenty four molecules in the system and a hydrogen gravimetric density of 7.1 wt%.**

hollow spaces compared to the other allotropes, allowing for more efficient packing of its square lithium adsorption sites within a certain area. Yet the lithium adsorption sites are not too close to each other, as in the adjacent hexa sites of the  $C_{64}$  structure, which can cause less stable hydrogen adsorption as well as impose geometrical constraints on hydrogen molecule packing. Hence, the  $C_{41}$  carbon allotrope seems to have a balanced structure with potential to be used in a practical hydrogen storage device. It should be noted the stated hydrogen gravimetric density is its theoretical best for the allotrope medium and in real life conditions and as part of a wider system the overall figure will likely drop somewhat. However, the structure will still likely produce hydrogen density in the ballpark of the DOE target value. Furthermore, the storage capacity of the structure may be even further enhanced by effects such as the presence of vacancies and other topological defects, which tend to increase hydrogen storage capability in graphene systems [28], and would be a good candidate for further investigation.

## Conclusions

The hydrogen storage capacity of six metal-decorated two-dimensional carbon allotropes ( $C_{65}$ ,  $C_{64}$ ,  $C_{63}$ ,  $C_{62}$ ,  $C_{31}$  and  $C_{41}$ ) was investigated using density functional theory. Multiple

positions on the allotrope structures were tested for double sided lithium decoration using LDA, GGA and vdW-DF2 functionals. Subsequently, the adsorption energy of a single hydrogen molecule on each lithium atom at these positions was determined using the same three functionals. All the structures were able to successfully bind lithium atoms with adsorption energies stronger than bulk lithium cohesive energy, with the exception of the  $C_{31}$  structure which had lithium adsorption energies significantly lower than the other allotropes. The remaining allotropes showed roughly similar lithium adsorption energies, with the  $C_{65}$  structure possessing the strongest binding energies. The vdW-DF2 functional resulted in the lowest lithium binding energies for all structures followed by the GGA functional, while the LDA functional produced the highest binding energies for all structures. All lithium decorated two dimensional allotropes successfully adsorbed hydrogen with stronger adsorption energies than for lithium decorated graphene. The GGA and vdW-DF2 hydrogen adsorption energies for all of the allotropes, except  $C_{31}$ , were roughly similar, while the LDA functional produced more widely fluctuating though generally stronger binding energies. In contrast to its lithium binding energies, the  $C_{31}$  structure had significantly stronger hydrogen binding energies than the other allotropes. The maximum possible hydrogen adsorption capacity of each carbon allotrope, other than  $C_{31}$ , was then examined using the vdW-DF2 functional alone. The  $C_{41}$  allotrope possessed an average hydrogen binding energy of 0.17 eV/ $H_2$  and produced the highest hydrogen gravimetric density at 7.12 wt%, better than that of metal decorated graphene, and was the only one to exceed the DOE hydrogen storage target.

## Acknowledgments

Computations were performed with support from Compute Canada supercomputing facilities SciNet HPC Consortium [32] and Calcul Qubec. Financial support for this work was provided by Natural Sciences and Engineering Research Council of Canada (NSERC), Connaught New Researcher Award and the University of Toronto. The authors gratefully acknowledge their support.

## REFERENCES

- [1] Satyapal Sunita, Petrovic John, Read Carole, Thomas George, Ordaz Grace. The u.s. department of energy's national hydrogen storage project: Progress towards meeting hydrogen-powered vehicle requirements. *Catal Today* 2007;120(34):246–56. Proceedings of the Korea Conference on Innovative Science and Technology (KCIST-2005): Frontiers in Hydrogen Storage Materials and Technology.
- [2] Office of Energy Efficiency Us Department of Energy, the FreedomCAR Renewable Energy, and Fuel Partnership. Targets for onboard hydrogen storage systems for light-duty vehicles. Department of Energy; SEPT 2009. p. 1–22.
- [3] Schlapbach Louis, Zuttel Andreas. Hydrogen-storage materials for mobile applications. *Nature* Nov 15 2001;414(6861):353–8. Copyright – Copyright Macmillan

- Journals Ltd. Nov 15, 2001; Last updated – 2013-01-28; CODEN – NATUAS.
- [4] Lim Kean L, Kazemian Hossein, Yaakob Zahira, Daud Wan RW. Solid-state materials and methods for hydrogen storage: a critical review. *Chem Eng Technol* FEB 2010;33(2):213–26. PT: J; TC: 14; UT: WOS:000275131500002.
  - [5] Goldsmith Jacob, Wong-Foy Antek G, Cafarella Michael J, Siegel Donald J. Theoretical limits of hydrogen storage in metalorganic frameworks: opportunities and trade-offs. *Chem Mater* 2013;25(16):3373–82.
  - [6] Liu Chang, Chen Yong, Wu Cheng-Zhang, Xu Shi-Tao, Cheng Hui-Ming. Hydrogen storage in carbon nanotubes revisited. *Carbon* 2010;48(2):452–5.
  - [7] Venkataraman Natarajan Sathiyamoorthy, Khazaei Mohammad, Sahara Ryoji, Mizuseki Hiroshi, Kawazoe Yoshiyuki. First-principles study of hydrogen storage over ni and rh doped [BN] sheets. *Chem Phys* 2009;359(13):173–8.
  - [8] Venkataraman Natarajan Sathiyamoorthy, Belosludov Rodion Vladimirovich, Note Ryunosuke, Sahara Ryoji, Mizuseki Hiroshi, Kawazoe Yoshiyuki. Theoretical investigation on the alkali-metal doped [BN] fullerene as a material for hydrogen storage. *Chem Phys* 2010;377(13):54–9.
  - [9] Spyrou Konstantinos, Gournis Dimitrios, Rudolf Petra. Hydrogen storage in graphene-based materials: efforts towards enhanced hydrogen absorption. *ECS J Solid State Sci Technol* 2013;2(10):M3160–9.
  - [10] Tozzini Valentina, Pellegrini Vittorio. Prospects for hydrogen storage in graphene. *NEST-Istituto Nanoscienze – Cnr and Scuola Normale Superiore*; 2012. p. 1–11.
  - [11] Wu Wenzhi, Guo Wanlin, Zeng Xiao Cheng. Intrinsic electronic and transport properties of graphyne sheets and nanoribbons. *Nanoscale* 2013;5:9264–76.
  - [12] Srinivasu K, Ghosh Swapan K. Graphyne and graphdiyne: promising materials for nanoelectronics and energy storage applications. *J Phys Chem C* 2012;116(9):5951–6.
  - [13] Jiao Yan, Du Aijun, Hankel Marlies, Zhu Zhonghua, Rudolph Victor, Smith Sean C. Graphdiyne: a versatile nanomaterial for electronics and hydrogen purification. *Chem Commun* 2011;47:11843–5.
  - [14] Zhang Hongyu, Zhao Mingwen, Bu Hongxia, He Xuijie, Zhang Meng, Zhao Lixia, et al. Ultra-high hydrogen storage capacity of li-decorated graphyne: a first-principles prediction. *J Appl Phys OCT 17 2012;112. 08435–084310.*
  - [15] Lu H, Li SD. Two-dimensional carbon allotropes from graphene to graphyne. *J Mater Chem C JAN 2013;1:3677–80.*
  - [16] Song Qi, Wang Bing, Deng Ke, Feng Xinliang, Wagner Manfred, Gale Julian D, et al. Graphenylene, a unique two-dimensional carbon network with nondelocalized cyclohexatriene units. *J Mater Chem C* 2013;1:38–41.
  - [17] Wang V, Mizuseki H, He HP, Chen G, Zhang SL, Kawazoe Y. Calcium-decorated graphene for hydrogen storage: a van der waals density functional study. *Comput Mater Sci APR 2012;55:180–5.*
  - [18] Zhou Weiwei, Zhou Jingjing, Shen Jingqin, Oujang Chuying, Shi Siqi. First-principles study of high-capacity hydrogen storage on graphene with li atoms. *J Phys Chem Solids 2012;73:245–51.*
  - [19] Lee Kyuho, Murray Eamonn D, Kong Lingzhu, Lundqvist Bengt I, Langreth David C. Higher-accuracy van der waals density functional. *Phys Rev B AUG 2010;82:081101.*
  - [20] Li Guo, Tamblyn Isaac, Cooper Valentino R, Gao Hong-Jun, Neaton Jeffrey B. Molecular adsorption on metal surfaces with van der waals density functionals. *Phys Rev B Mar 2012;85:121409.*
  - [21] Giannozzi P, Baroni S, Bonini N, Calandra M, Car R, Cavazzoni C, et al. Quantum espresso: a modular and open-source software project for quantum simulations of materials. *J Phys Condens Matter* 2009;21:395502.
  - [22] Perdew John P, Wang Yue. Accurate and simple analytic representation of the electron-gas correlation energy. *Phys Rev B Jun 1992;45:13244–9.*
  - [23] Perdew JP, Burke K, Ernzerhof M. Generalized gradient approximation made simple. *Phys Rev Lett* 1996;77(18):3865–8.
  - [24] Dion M, Rydberg H, Schroder E, Langreth DC, Lundqvist BI. Van der waals density functional for general geometries. *Phys Rev Lett Jun 2004;92(24):246401.*
  - [25] Monkhorst HJ, Pack JD. Special points for brillouin-zone integrations. *Phys Rev B* 1976;13(12):5188–92.
  - [26] Methfessel M, Paxton AT. High-precision sampling for brillouin-zone integration in metals. *Phys Rev B AUG 1989;40:3616–21.*
  - [27] Dai Jiayu, Yuan Jianmin, Giannozzi Paolo. Gas adsorption on graphene doped with b, n, al, and s: a theoretical study. *Appl Phys Lett* 2009;95(23):232105.
  - [28] Yadav Shwetank, Zhu Zhihui, Singh Chandra Veer. Defect engineering of graphene for effective hydrogen storage. *Int J Hydrogen Energy* 2014;39(10):4981–95.
  - [29] Bhattacharya A, Bhattacharya S, Majumder C, Das GP. Transition-metal decoration enhanced room-temperature hydrogen storage in a defect-modulated graphene sheet. *J Phys Chem C* 2010;114(22):10297–301.
  - [30] Berland Kristian, Hyldgaard Per. Analysis of van der waals density functional components: binding and corrugation of benzene and c<sub>60</sub> on boron nitride and graphene. *Phys Rev B May 2013;87:205421.*
  - [31] Wong Jasmine, Yadav Shwetank, Tam Jasmine, Singh Chandra Veer. A van der waals dft comparison of metal decorated graphene systems for hydrogen adsorption. *J Appl Phys* 2014;115(23).
  - [32] Loken Chris, Gruner Daniel, Groer Leslie, Peltier Richard, Bunn Neil, Craig Michael, et al. Scinet: lessons learned from building a power-efficient top-20 system and data centre. *J Phys Conf Ser* 2010;256:012026.